An Efficient Wireless Power Transfer System To Balance the State of Charge of Electric Vehicles

Ankur Sarker[◇], Chenxi Qiu[◇], Haiying Shen[◇], Andrea Gil[†], Joachim Taiber[†],
Mashrur Chowdhury[‡], Jim Martin[§], Mac Devine[♯] and AJ Rindos[♯]
[◇]*Department of Electrical and Computer Engineering, Clemson University, Clemson, SC 29634*
[†]*International Center for Automotive Research, Clemson University, Greenville, SC 29607*
[‡]*Department of Automotive Engineering, Clemson University, Clemson, SC 29634*
[†]*School of Computing, Clemson University, Clemson, SC 29634*
[♯]*IBM, Research Triangle Park, Durham, NC 27709*
{[◇]*asarker,* [◇]*chenxiq,* [◇]*shenh,* [†]*agil,* [†]*jtaiber,* [‡]*mac,* [§]*jmarty*}*@clemson.edu*
{[♯]*wdevine,* [♯]*rindos*}*@us.ibm.com*

***Abstract*—As an alternate form in the road transportation system, electric vehicle (EV) can help reduce the fossil-fuel consumption. However, the usage of EVs is constrained by the limited capacity of battery. Wireless Power Transfer (WPT) can increase the driving range of EVs by charging EVs in-motion when they drive through a wireless charging lane embedded in a road. The amount of power that can be supplied by a charging lane at a time is limited. A problem here is when a large number of EVs pass a charging lane, how to efficiently distribute the power among different penetrations levels of EVs? However, there has been no previous research devoted to tackling this challenge. To handle this challenge, we propose a system to balance the State of Charge (called BSoC) among the EVs. It consists of three components: i) fog-based power distribution architecture, ii) power scheduling model, and iii) efficient vehicle-to-fog communication protocol. The fog computing center collects information from EVs and schedules the power distribution. We use fog closer to vehicles rather than cloud in order to reduce the communication latency. The power scheduling model schedules the power allocated to each EV. In order to avoid network congestion between EVs and the fog, we let vehicles choose their own communication channel to communicate with local controllers. Finally, we evaluate our system using extensive simulation studies in Network Simulator-3, MatLab, and Simulation for Urban MObility tools, and the experimental results confirm the efficiency of our system.**

***Keywords*-Electric vehicle; Transportation system; Wireless power transfer; In-motion power transfer**

I. Introduction

Intelligent Transportation System (ITS) utilizes traffic information, communication, and computing capabilities and it provides an integrated system consisting of people, roads, and vehicles to increase traffic efficiency and decrease traffic congestion. As a component of the future generation ITS, the design and implementation of Electric Vehicles (EVs) have drawn much attention in recent years. Several works have already been demonstrated the future impact of EVs on a road transportation system [1–4] such as economical energy consumption and environment protection. In an EV, the onboard battery supplies the energy demands of the vehicle. However, EVs have some battery-related issues such as heavy weight, long charging time, large size, and short driving range. To alleviate these problems, wireless charging or *Wireless Power Transfer* (WPT) technique arise. It makes the charging procedures more convenient by allowing charging procedure take place automatically without having any physical contact between utility power supply and electric battery. It transfers power from grid to an EV's battery while it is moving through a charging lane embedded in a road. An EV spends very little time on top of the charging coils. The shorter duration of time requires higher power levels in charging infrastructure so that higher amount of power can be transferred. However, the investment for charging infrastructure goes up to meet the demand for higher power. Therefore, the amount of power that can be supplied by a charging lane at a time is always limited. A problem here is *when a large number of EVs pass a charging lane, how to efficiently distribute the power among them when the infrastructure is not able to fulfill all the demands?* However, there has been no previous research devoted to tackling this challenge.

To handle this challenge, in this paper, we propose a dynamic WPT system to balance the State of Charge (called BSoC) among the EVs passing a charging section. None of the previous works [5–8] try to distribute power from grid to heterogeneous EVs considering their SOCs. BSoC consists of three components: i) fog-based power distribution architecture, ii) power scheduling model, and iii) efficient vehicle-fog communication protocol. As shown in Fig. 1, in BSoC, a fog is a computer cluster that functions as grid side controller (GSC) that monitor power distribution among EVs [9, 10]. The fog-based GSC collects information from EVs and schedules the power distribution among the EVs. We choose fog closer to vehicles rather than cloud [11] in order to reduce the communication latency. The power scheduling model schedules the power allocated to each EV

from charging sections based on the number of vehicles and their SOCs present at a particular time. In order to reduce network congestion between EVs and the fog-based GSCs, we let vehicles choose their own communication channel to communicate with the GSC. In this way, EVs do not have to use the CSMA/CA technique and can avoid the exposed terminal problem, in which an EV cannot send messages due to signal interference with the transmissions of its neighboring EVs.

- Fog-based power distribution architecture. To ensure scalability, we develop a hierarchical system, which consists of *Global Charging Controller* (GCC), GSCs and EVs in three top-down levels. GCC is located in a cloud and it receives vehicles' information and distributes power from power grid to GSC-controlled charging sections accordingly. Each local GSC monitors charging sections in a charging lane installed on top of route segments. It collects information from vehicles, processes vehicles' information, and schedules and distributes power from charging sections to EVs. In our system, GSCs are fog-enabled modules and they are located closer to EVs, which help reduce communication latency between EVs and GSCs.
- Power scheduling model. The power scheduling model is used by a GSC to schedule the power for each EV passing each charging section in a charging lane. The model aims to balance the SOC of EVs passing a charging lane by taking consideration of vehicle's energy model, and heterogeneous vehicles' parameters. We formulate the power scheduling problem as a convex optimization problem where heterogeneous vehicles' parameters are considered as constraints and use the subgradient method to solve the formulated problem.
- Efficient vehicle-to-fog communication protocol. It is important to achieve low-latency vehicle-to-fog communication, so that EVs can receive power in time. To reduce the communication delay, each EV uses Dedicated Short Range Communication (DSRC) based wireless communication for vehicle-to-GSC (V2G) communication in our system. IEEE 802.11p-based DSRC uses one control and six service channels to reduce network congestion. However, it uses Carrier Sense Multiple Access with Collision Avoidance (CSMA/CA) technique which exhibits poor performance in high traffic density and also suffers by exposed terminal problem as EVs need to wait for their neighbor EVs to send messages [12]. It means the communication procedures between vehicles and controllers may exhibit poor performance. However, our dynamic WPT system is dependent on the availability and the prompt analysis of the EVs' information (e.g., number of vehicles, SOCs, locations, etc) with low latency. To alleviate the channel congestion during the communication procedure between GSC and EVs, we let each vehicle to decide its own communication channel based on its distance from GSC. We divide the coverage area of GSC into six regions. EVs pick their communication channels based on the regions they are residing at a particular time. After getting the messages from EVs in a particular channel, GSC can also determine the EVs in each region accordingly. Since a particular band of channel is capable of handling 10–15 nodes at one time, our system does not have to use the CSMA/CA technique. As a result, network congestion is reduced even with the presence of a large number of EVs. Since each EV does not need to wait for other EVs to complete transmitting messages, it can also help to reduce transmission latency without causing the exposed terminal problem).

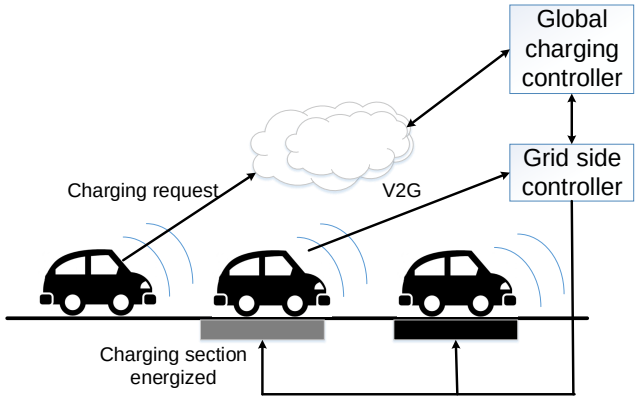

Figure 1: The system architecture.

We evaluate our system using Network Simulator-3 (NS-3), MatLab, and Simulation on Urban MObility (SUMO) tools to get realistic evaluation results in different aspects. From the experiment, we find that our fog-based computation architecture causes lower communication latency than other cloud-based architecture. Our proposed power scheduling model achieves more balanced SOC of EVs in comparison with other power distribution schedules. Further, our efficient vehicle-to-fog communication protocol causes less network congestion and lower packet drop rate than existing time division multiplexer (TDM) protocol.

The rest of paper is organized as follows. Section II describes our proposed BSoC system. Then, Section III presents the evaluation of the proposed BSoC WPT system using extensive simulation study. Section IV presents an overview of related work. Finally, Section V concludes the paper with remarks on our future work.

II. Design of the BSoC System

In this section, we present the three components of our proposed BSoC WPT system. Specifically, Section II-A presents the fog-based power distribution architecture, Section II-B presents the power scheduling model, and Section II-C presents the efficient vehicle-to-fog communication protocol to address the shortcoming of existing CSMA/CA technique used in DSRC protocol.

A. Fog-based Power Distribution Architecture

A *charging lane* is the portion of the road that contains one or more charging sections. A *charging section* is a portion of a road that has charging coils embedded and EVs can be charged by running on top of the charging section. Each charging section has a specific starting point and ending point. The maximum amount of energy that a charging section can provide to an EV is determined by the power rate of the charging coil and the time that the vehicle spends on top of the charging section. Additionally, when serving multiple vehicles, each charging section can deliver no more than the maximum power rate. In consequence, without any intelligence added, the charging section can only serve a fixed amount of vehicles when there are a large number of EVs passing the charging section and their demands exceed the maximum power rate. For a given vehicle speed, the amount of energy that a charging lane can supply equals the sum of the energy that each charging section provides for that particular velocity.

There is a local controller *GSC* associated with several charging sections in a charging lane. The GSC monitors the charging sections and it also distributes the power in a particular charging section at every point of time. The GSC is able to communicate with the nearby vehicles via DSRC communication device and it is aware of the number of vehicles that are on top of its respective charging section. The *GCC* is connected with several GSCs and it determines the power distribution from power grid to GSCs. EVs may send the charging request to GCC and GCC may accept or deny the request based on its current load.

Our fog-based power distribution architecture is a hierarchical WPT system, where GCC is on the top, GSCs constitute the middle level and the EVs constitute the bottom level. GCC is located in a cloud and GSCs are located in fogs and each fog is a cluster. We use fog rather than cloud because fog is closer to EVs, which can reduce the communication latency. EVs send their information to GCC, which schedules the power distribution among GSCs. Each GSC receives information from EVs and schedules the power distribution among charging sections or EVs. In this paper, we assume that there is only one EV on a charging section at a time.

Each vehicle has a unique vehicle ID. When an EV enters the coverage area of a particular GSC, the vehicle sends its status information (e.g., SOC, velocity, position, traveling route) to that GSC. When a vehicle needs to be charged, it sends a charging request to the fog-based GSC. Then, GSC processes the information and runs the power scheduler periodically to determine the power distribution from each charging section. Fog computing allows real-time data processing and data delivery, especially for delay sensitive services such as wireless power transfer scheduling for EVs. The fog computes the schedule of the power distribution among the charging sections, that is, the power to each charging section at every point of time. The fog can also compute the projected travel time, remaining SOC to reach charging sections for each vehicle. Fog-based GSC also ingests the data generated by charging sections such as charging status related to their maintenance and control operations. Periodically, fog-based GSC uploads the status information to GCC so that GCC can learn the statuses of charging sections. In the following, we present the power scheduling model that each GSC uses to schedule the power distribution among charging sections in a charging lane.

B. Power Scheduling Model

The power scheduling computation is performed by the fog. A GSC periodically collects EVs' information and uses the power scheduling model to calculate the power distribution among the charging sections (or to the EV on each charging section). First, we consider a scenario where there are m EVs traveling through a route with a GSC, and the entering time to and the leaving time from a charging lane of each vehicle i ($1 \leq i \leq m$) are denoted by t_i^{s} and t_i^{e}, respectively. Considering that EVs are continuously entering the charging lane, the GSC identifies the vehicles on the charging lane at the same time and balances these vehicles' SOC when they leave the charging lane. The route is installed with n charging sections $c_1, ..., c_n$ to charge the vehicles based on their current stored energy to balance their SOC. Here, the charging sections are uniformly distributed and their intermediate distances are the same. The maximum capacity of a GSC is A and the capacity of each charging section j is a_j. We represent the time that each vehicle i arrives c_j by $t_{i,j}$. We use $y_i(t)$ to represent the SOC in vehicle i at time t, and let $y(t) = [y_1(t)y_2(t)...y_m(t)]^\top$. Then, $y_i(t_i^s)$ and $y_i(t_i^e)$ represent the SOC of vehicle i when it enters and leaves the charging lane, respectively. Table I and Table II present the notations and definitions.

In the following part, we will describe the power consumption model, which is used to calculate the SOC of each EV i. First, the energy consumption of EV i at each time slot, denoted by $P_{\mathrm{trac},i}$, is calculated by [13]

$$P_{\mathrm{trac},i} \quad = \quad M_i a_i v_i + \frac{1}{2}\rho_{\mathrm{air},i} C_{\mathrm{d},i} v_i^3 \qquad (1)$$

where M_i, a_i, v_i, $\rho_{\mathrm{air},i}$, and $C_{\mathrm{d},i}$ represent the *mass*, the *acceleration*, the *velocity*, the *air density*, and *the drag coefficient* of EV i, respectively. The EV's battery power,

Table I: Symbols and Definitions.

Symbol	Definition
m	The number of EVs
t_i^s	The start time of EV i
t_i^e	The end time of EV i
n	The number of charging sections
c_j	The jth charging section
a_j	The maximum power that can be provided by the charging section j
A	The maximum power that can be provided by the GSC
$y_i(t)$	The SOC of EV i at time t
z_i	The rated battery capacity of EV i

denoted by $P_{\mathrm{batt},i}$, is given by [13]

$$P_{\mathrm{batt},i} = \frac{P_{\mathrm{add},i}}{\eta_{\mathrm{PT},i}} - P_{\mathrm{trac},i}, \tag{2}$$

where $P_{\mathrm{add},i}$ represents the power added to EV i's battery and $\eta_{\mathrm{PT},i}$ represents the transmission efficiency of EV i. Since the power from charging section cannot be 100% transferred to EVs, $\eta_{\mathrm{PT},i}$ is always higher than 1. Also, we use $I_i(t)$ [13] to represent the current of EV i at time t delivered by the battery, which is given by

$$I_i(t) = \frac{V_{\mathrm{oc},i} - \sqrt{V_{\mathrm{oc},i}^2 - 4R_{\mathrm{int},i}z_i(t)}}{2R_{\mathrm{int},i}}, \tag{3}$$

Here, $V_{oc,i}(t)$ represents an ideal voltage source connected in series with the battery internal resistance $R_{int,i}$ for vehicle i and the battery power is $P_{batt,i}$ [13].

$$\begin{aligned} y_i(t+1) &= y_i(t) - \frac{1}{x_j(t)}\int_t^{t+1} I_i(t)dt \\ &= y_i(t) - \frac{I_i(t)}{Q_{\mathrm{batt},i}} \\ &= y_i(t) - \frac{V_{\mathrm{oc},i} - \sqrt{V_{\mathrm{oc},i}^2 - 4R_{\mathrm{int},i}z_i(t)}}{2R_{\mathrm{int},i}Q_{\mathrm{batt},i}}. \end{aligned} \tag{4}$$

where we assume $I_i(t)$ is constant during $[t, t+1]$ and $x_j(t)$ denotes the power allocated to the charging section j, which is the charging section that EV i is located in at time t. Here, $y_i(t)$ is calculated by integrating the current and comparing that value with the rated battery capacity z_i of the entire battery pack. The charge transferred to the battery is obtained by as follows [13]:

$$y_i(t+1) = y_i(t) - \frac{1}{Q_{batt}}\int_t^{t+1} I_i(t)dt \tag{5}$$

where $I_i(t)$ denotes the current, which is calculated by [13]

$$I_i(t) = \frac{V_{oc,i} - \sqrt{V_{oc,i}^2 - 4R_{int,i}P_{batt,i}}}{2R_{int,i}} \tag{6}$$

From Equ. (5) and (6), we can further derive $y_i(t+1)$ as follows:

$$y_i(t+1) = \frac{y_i(t) - I_i(t)}{2R_{int,i}} \tag{7}$$

Now, the problem is to distribute the power to each charging section to guarantee all the vehicles have same SOC when they leave the charging lane. If vehicle i reaches a charging section, say j, then the y_i stored in its battery should be $\frac{y_i(t)-I_i(t)}{2R_{int,i}}$; otherwise, it is same. We can consider $x_j(t)$ as the power distributed from charging section j to one vehicle at time t. Finally, our objective is to balance the SOC of all vehicles when they leave the charging lane:

$$\min \sum_{i=1}^{m}\left(y_i(t_i^{\mathrm{e}}) - \frac{\sum_{j=1}^{m} y_j(t_i^{\mathrm{e}})}{m}\right)^2. \tag{8}$$

or we can write Equ. (8) as

$$\min \ \mathbf{y}^\top(t_i^{\mathrm{e}})\mathbf{N}\mathbf{N}^\top\mathbf{y}(t_i^{\mathrm{e}}) \tag{9}$$

where $\mathbf{N} \in \mathbb{R}^{n\times n}$ is defined by

$$\mathbf{N} = \begin{bmatrix} 1 & -\frac{1}{n} & \cdots & -\frac{1}{n} \\ -\frac{1}{n} & 1 & \cdots & -\frac{1}{n} \\ \vdots & \vdots & \ddots & \vdots \\ -\frac{1}{n} & -\frac{1}{n} & \cdots & 1 \end{bmatrix}.$$

Besides achieving the objective function Equ. (9), we also need to satisfy the following constraints:

$$\sum_{j=1} x_j(t) \le A, \ \forall j, t \tag{10}$$

$$x_j(t) \le a_j, \ \forall j, t \tag{11}$$

$$y_i(t) \le 1, \ \forall t, i \tag{12}$$

$$z_i(t+1) = \begin{cases} z_i(t) - P_{\mathrm{trac},i} & \text{if } t \notin \mathcal{T}_i \\ z_i(t) + \frac{x_j(t)}{\eta_{\mathrm{PT},i}} - P_{\mathrm{trac},i} & \text{if } t = t_{i,j} \end{cases} \tag{13}$$

where the first constraint Equ. (10) means that the sum of the allocated power of all the charging sections cannot exceed the maximum power provided by GSC. The second constraint Equ. (11) means that the power allocated to each charging section j cannot exceed the maximum power provided by the charging section j in each time point. The third constrain Equ. (12) means that the SOC of each EV i cannot exceed 1 and the fourth constraints Equ. (13) means that, at time t, 1) if EV i is not located at any charging section, then its power is reduced by $P_{\mathrm{trac},i}$; otherwise, if EV i is located at a charging section, then its energy is added by $x_j(t) - P_{\mathrm{trac},i}$. In what follows, we will prove that the scheduling problem defined by Equ. (9) - Equ. (13) is a convex problem, i.e., the Hessian matrices of Equ. (9) – (13) are nonnegative definite [14]. First, the Hessian matrix

Table II: EVs' Parameters and Definitions.

Parameter	Definition
$Q_{\mathrm{batt},i}$	The battery capacity of EV i
$I_i(t)$	The current of EV i at time t
$V_{\mathrm{oc},i}$	The voltage source of EV i
$R_{\mathrm{int},i}$	The internal battery resistance of EV i
$P_{\mathrm{batt},i}$	EV i's battery power
$P_{\mathrm{batt},i}^{\max}$	The maximum power of battery of EV i
$P_{\mathrm{add},i}$	The power added to EV i's battery
$\rho_{\mathrm{air},i}$	The air density of EV i
$C_{\mathrm{d},i}$	The drag coefficient of EV i
$A_{\mathrm{f},i}$	The frontal area of EV i
M_i	The mass of EV i
$C_{\mathrm{r},i}$	The rolling resistance coefficient of EV i
$\eta_{\mathrm{PT},i}$	The transmission efficiency of EV i
$\eta_{\mathrm{GB},i}$	The gearbox efficiency of EV i
$\eta_{\mathrm{EM},i}$	The electric motor efficiency of EV i
L_j	The length of charging section j

of the objective function (Equ. (9)) is

$$\begin{aligned}\mathbf{H}_{f(\mathbf{y}^\top(t_i^{\mathrm{e}}))} &= \begin{bmatrix} \frac{\partial^2 f}{\partial y_1(t_i^{\mathrm{e}})^2} & \cdots & \frac{\partial^2 f}{\partial y_1(t_i^{\mathrm{e}})\partial y_n(t_i^{\mathrm{e}})} \\ \vdots & \ddots & \vdots \\ \frac{\partial^2 f}{\partial y_1(t_i^{\mathrm{e}})\partial y_n(t_i^{\mathrm{e}})} & \cdots & \frac{\partial^2 f}{\partial y_n(t_i^{\mathrm{e}})^2} \end{bmatrix} \\ &= \mathbf{N}\mathbf{N}^\top, \end{aligned} \tag{14}$$

which is nonnegative definite since for each $\mathbf{x} \in \mathbb{R}^m$, $\mathbf{x}^\top\mathbf{N}\mathbf{N}^\top\mathbf{x} \geq 0$ [14].

Then, we consider the constraint functions. The constraints Equ. (10) - Equ. (12) are all linear functions, which indicates that their Hessian matrices are all zero matrix and hence nonnegative definite. Now, we need to prove the convexity of Equ. (13). To this end, we first need to write Equ. (13) in quadratic form [14]. The detailed process to derive its quadratic form is shown as follows.

Based on Equ. (6) and Equ. (7), we have:

$$\begin{aligned} & -\sqrt{V_{\mathrm{oc},i}^2 - 4R_{\mathrm{int},i}z_i(t)} \\ = \;& y_i(t)2R_{\mathrm{int},i}Q_{\mathrm{batt},i} - y_i(t+1)2R_{\mathrm{int},i}Q_{\mathrm{batt},i} - V_{\mathrm{oc},i}. \end{aligned} \tag{15}$$

from which we can derive that

$$z_i(t) = \mathbf{w}_i^\top(t)J\mathbf{w}_i(t) + \mathbf{b}^\top\mathbf{w}_i(t), \tag{16}$$

where

$$J = \begin{bmatrix} -R_{\mathrm{int},i}Q_{\mathrm{batt},i}^2 & R_{\mathrm{int},i}Q_{\mathrm{batt},i}^2 \\ R_{\mathrm{int},i}Q_{\mathrm{batt},i}^2 & -R_{\mathrm{int},i}Q_{\mathrm{batt},i}^2 \end{bmatrix},$$

$$\mathbf{b} = \begin{bmatrix} Q_{\mathrm{batt},i}V_{\mathrm{oc},i} \\ -Q_{\mathrm{batt},i}V_{\mathrm{oc},i} \end{bmatrix}, \text{ and } \mathbf{w}_i(t) = \begin{bmatrix} y_i(t) \\ y_i(t+1) \end{bmatrix}.$$

Then, according to Equ. (16), we can rewrite Equ. (13) as Equ. (17) - (18):
If $t \notin \mathcal{T}_i$,

$$\begin{aligned} & \mathbf{w}_i^\top(t+1)J\mathbf{w}_i(t+1) + \mathbf{b}^\top\mathbf{w}_i(t+1) \\ = \;& \mathbf{w}_i^\top(t)J\mathbf{w}_i(t) + \mathbf{b}^\top\mathbf{w}_i(t) - P_{\mathrm{c}} \end{aligned} \tag{17}$$

If $t \in \mathcal{T}_i$ and $t = t_{i,j}$

$$\begin{aligned} & \mathbf{w}_i^\top(t+1)J\mathbf{w}_i(t+1) + \mathbf{b}^\top\mathbf{w}_i(t+1) \\ = \;& \mathbf{w}_i^\top(t)J\mathbf{w}_i(t) + \mathbf{b}^\top\mathbf{w}_i(t) + x_j(t) - P_{\mathrm{c}} \end{aligned} \tag{18}$$

As we have derived the quadratic form of Equ. (13) shown in Equ. (17) – (18), in which the Hessian matrix is J. Because J is nonnegative definite since for any vector $[x_1, x_2]^\top$ $(x_1, x_2 \in \mathbb{R})$, we have

$$\begin{aligned} & [x_1, x_2]J[x_1, x_2]^\top \\ = \;& R_{\mathrm{int},i}Q_{\mathrm{batt},i}^2x_1^2 - 2R_{\mathrm{int},i}Q_{\mathrm{batt},i}^2x_1x_2 \\ + \;& R_{\mathrm{int},i}Q_{\mathrm{batt},i}^2x_2^2 \\ = \;& R_{\mathrm{int},i}Q_{\mathrm{batt},i}^2\left(x_1 - x_2\right)^2 \geq 0. \end{aligned} \tag{19}$$

Thus, the scheduling problem is convex. To solve the problem defined by Equ. (9) – (13), in fog, our system uses the subgradient method, which is an iterative method to solve convex minimization problems [14].

Algorithm 1 Pseudocode of the subgradient method.

Input: Parameters of all the EVs
Output: $\mathbf{w}^*$ ▷ *Power allocation of all charging sections.*
1: Select a starting solution: $\mathbf{w}^{(1)} = \mathbf{0}$
2: Put $k = 1$
3: **for** $\xi^{(k)}(\mathbf{w}^{(k)}) < \epsilon$ **do**
4: $\quad\xi^{(k)}(\mathbf{w}^{(k)}) = \nabla f(\mathbf{w}^{(k)})$
5: $\quad$**if** $\xi^{(k)}(\mathbf{w}^{(k)}) = 0$ **then**
6: $\quad\quad$Break
7: $\quad$**else**
8: $\quad\quad$Select a step size $\alpha^{(k)} > 0$
9: $\quad\quad$compute $\mathbf{w}^{(k+1)} \leftarrow \mathbf{w}^{(k)} + \alpha^{(k)}\xi^{(k)}(\mathbf{w}^{(k)})$
10: $\quad$**end if**
11: $\quad k = k + 1$
12: **end for**
13: $\mathbf{w}^* \leftarrow \mathbf{w}^{(k)}$
14: **return** $\mathbf{w}^*$

Algorithm 1 shows the pseudo code of the subgradient method: Here $\mathbf{w}^{(k)}$ is the k^{th} iterate, $\xi^{(k)}(\mathbf{w}^{(k)})$ is the subgradient of f at $\mathbf{w}^{(k)}$, and $\alpha^{(k)} > 0$ is the kth step size. At the beginning, we initiate $\mathbf{w}^{(1)}$ by $\mathbf{0}$ and set k by 1 (line 1–2). Then, in each iteration, we first derive the subgradient of $f(\mathbf{w}^{(k)})$ (line 4). If $\xi^{(k)}(\mathbf{w}^{(k)}) = 0$, which indicates that $\mathbf{w}^{(k)}$ is the global optimal solution, the algorithm is finished; otherwise, we take a step in the direction of a negative subgradient $\alpha^{(k)}\xi^{(k)}(\mathbf{w}^{(k)})$. The above process is repeated until $\xi^{(k)}(\mathbf{w}^{(k)}) < \epsilon$, i.e., the subgradient is close to 0.

C. Efficient Vehicle-Fog Communication Protocol

In our WPT system, we use the IEEE Wireless Access in Vehicular Environment (WAVE) set of standards for the V2G

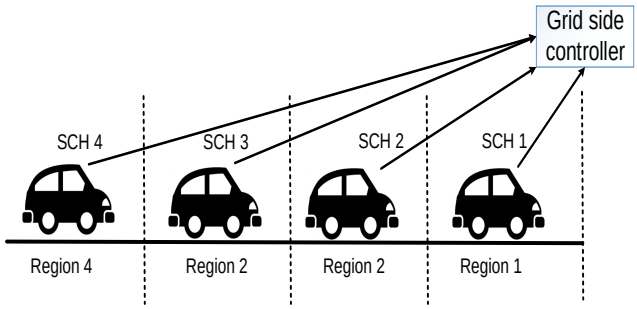

Figure 2: Channel allocation.

communication where the communication range of DSRC device is approximately 500–1000m. In the following, we introduce the shortcoming of the CSMA/CA technique used in the existing DSRC protocol and then we propose our strategy to overcome the shortcoming.

WAVE includes the physical and link layer access methods (defined by IEEE 802.11p) and all a range of protocols and services (defined by the IEEE 1609 protocols suite) to support connected vehicle applications and IEEE 1609 protocol suite. DSRC manages access application access to seven 10MHz channels operating at 5.9Gz. These seven channels consist of one CCH (Control Channel), four SCHs (Service Channels), and two other channels for high power and accident avoidance. The 802.11p standard extends the basic service set with the Enhanced Distributed Channel Access (EDCA) mechanism for classifying different data flow into different access categories. The hidden terminal problem arises in DSRC-based wireless communication, when two or more nodes hidden from each other try to access the communication channel at the same time and then the transmission signals interfere with each other and produce channel congestion. To deal with hidden terminal problem, IEEE 802.11p utilizes the CSMA/CA mechanism, the signal overhead on the control channel due to the handshaking procedures could penalize the critical messages. Besides, the CSMA/CA mechanism may show poor performance with heavy packet loss and average delay in coarse traffic scenario [12]. The CSMA/CA also introduces the exposed terminal problem where nearby nodes may wait for one particular node to finish its transmission. Moreover, DSRC is pushed to the limit if different application scenarios (e.g., collision-warning function, longitude control, safety, cooperative assistance, etc), which create contradictory constraints under heavy network traffic conditions.

To provide a more robust wireless network, we make the following extensions. In our system, we let EVs to choose their own channel to communicate with GSC avoiding the overhead caused by CSMA/CA and providing a solution to the exposed terminal problem. An EV chooses its communication channel based on the distance between itself and GSC. In current DSRC system, there are seven channels available to use for EVs. Here, we use the frequency division multiplexing (FDM) approach to allocate the channels to EVs. We let EVs and GSC to use one CCH channel for control applications, node discovery, and etc.

In case of node discovery, the GSC periodically sends a beacon message including information such as current position, charging sections status and charging sections positions, and amount of power offering. When an EV enters inside the communication region of GSC, it receives the beacon message and selects a service channel based on its distance from the GSC. For example, assuming six service channels are available and that the communication range of a GSC is 600m, EVs are grouped into 6 regions based on location (as illustrated in Fig. 2). After receiving a beacon message from the GSC in CCH channel, EVs will respond with an acknowledgment message containing its ID, SOC, destination, and charging request over the selected service channel. Based on the acknowledgments received from EVs, GSC can decide how many EVs are in each region. If the total power demands of EVs are more than the power capacity of the charging lanes, GSC process the messages for the power distribution scheduling. When the power allocation schedule for EVs is decided in the fog, the GSC sends messages via the CCH channel to let all EVs know that their charging requests have been processed. After the notification message from GSC in CCH channel, the EVs selected for being charged do not need to send any request again to GSC.

III. Performance Evaluation

A. Experimental Settings

In this section, we evaluate the performance of our proposed BSoC WPT system with other methods in three aspects: fog-based power distribution architecture, power scheduling model, and vehicle-to-fog communication protocol explained below.

Fog-based power distribution architecture. We choose existing cloud-based GTES [15] where each EV periodically sends their status information and energy requirements to the cloud-based GSC and then, based on the received information, the GSC runs the centralized game theoretic energy schedule algorithm to distribute the energy to users. We used NS-3 to simulate the scenario having various child nodes as EVs with a fog-based or cloud-based parent node as GSC. In the NS-3 experiment, We used 50 EVs as mobile nodes. In order to simulate the fog-based transmission latency and cloud-based transmission latency in our experiment, we considered DSRC-based fog node as GSC and LTE-based cloud node as GSC, respectively. We tested the latency of transmitting 128 byte data packets between GSC and EVs, We then recorded the transmission latencies and calculated the average values.

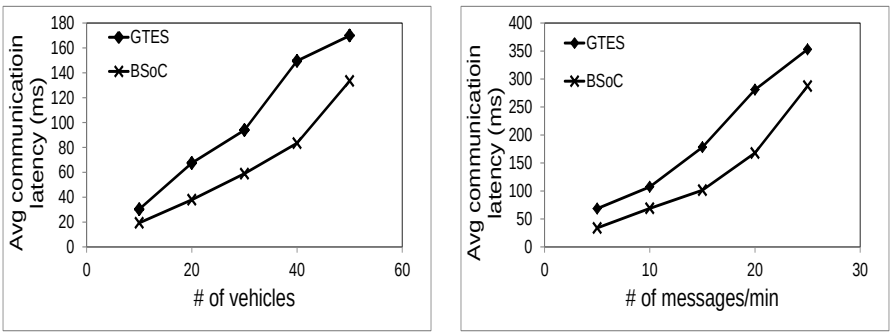

(a) Latency vs. number of vehicles (b) Latency vs. message sending frequency

Figure 3: Comparison between fog-based BSoC and cloud-based GTES.

Table III: EVs' Parameters [16–18].

Parameters	Nissan Leaf	Toyota Prius	Chevy Volt
Drag Coefficient C_d	1	1	1
Vehicle frontal area A_f $[m^2]$	0.725	0.576	0.622
Vehicle Mass M $[kg]$	1521	1380	1607
Rolling Ressistace Coefficient C_r	0.02	0.02	0.02
Transmission Efficiency η_{tx}	0.98	0.98	0.98
Gearbox Efficiency η_{GB}	0.98	0.98	0.98
Electric Motor Efficiency η_{EM}	0.99	0.99	0.99

Power scheduling model. We choose the "Equal Share" and "First Come First Serve" (FCFS) methods for comparing the power scheduling performance with our BSoC System. In Equal Share, suppose there are m vehicles on top of the charging section at a particular time, the amount of power that each EV is scheduled to receive is A/m. In FCFS, each EV's battery is fully charged and EVs are scheduled to receive power in the order that they arrive at the charging section. Here, we used MatLab to get the solution of our power scheduling optimization problem, and then we used SUMO to apply the solution in the realistic traffic scenario. For the simulation, we fixed 10–50 EVs and 10 charging sections. Three types of EVs were considered (Nissan Leaf, Toyota Prius, and Chevy Volt) in our experiment. Table III shows the parameters of EVs. Besides, we set the length, maximum capacity, and coil capacity of charging section to 200m, 600kw, and 100kw, respectively.

Vehicle-to-fog communication protocol. In vehicular network perspective, we conducted experiment with and without our channel allocation technique in current IEEE 802.11p protocol. In current protocol, it uses time division multiplexing (TDM) to reduce network congestion. The access point (AP) divides the timeline into contiguous synchronization intervals, each of which consists of a fixed CCH interval (TCCH) and a fixed SCH interval (TSCH). There is a guard interval (g) at the beginning of each channel interval is used to switch from one channel to another. The default intervals of each channel is set to 50ms. In this scenario, we evaluated the performance of our channel allocation technique using NS-3 where we considered EVs and GSC were equipped with DSRC communication devices which had about 500m communication range. we used 10–50 moving nodes with single AP as GSC. This is reasonable considering the communication range of DSRC (i.e., 500m-1000m) and the inter-vehicle distance (i.e., 40m-80m).

B. Experimental Results

Fog-based power distribution architecture. Fig. 3(a) and Fig. 3(b) show the experiment results from NS-3. Here, we compared our BSoC's fog computing performance with GTES's cloud computing performance. To do the comparison between BSoC and GTES, we calculated the average communication latency by varying the number of EVs and message sending frequency. We refer to the *average communication latency* as the average time it takes for a transmitted packet to be received by the GSC from EVs. Fig. 3(a) shows the average communication latency when the number of EVs was varied from 10 to 50 and each EV sends 20 packets per minute. We see that when the number of EVs increases, the average communication latency of cloud-based GTES increased drastically. However, in our fog-based BSoC, the increase rate with respect to the number of EVs is not that high. In GTES, EVs send message directly to the cloud-based GSC using LTE signal. On the other hand, EV sends the message to fog-enabled local GSC using DSRC signal in our BSoC system. The DSRC data transmission rate is faster and it is less affected by the channel congestion than LTE data transmission rate [19]. Thus, the average computation latency is not increased drastically in our fog-enabled BSoC system. Fig. 3(b) shows the average communication latency when we varied the packet transmission frequency and there were 30 EVs. We make the same observation that the average communication latency in BSoC is lower than GTES due to the same reasons. From the discussion, we can interpret the fog-based BSoC outperforms than cloud-based

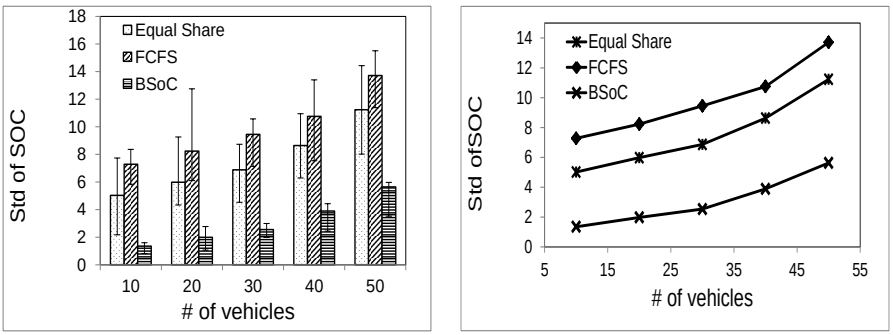

(a) Std of SOC with errors

(b) Std of SOC

Figure 4: Comparison between Equal Share, FCFS, and BSoC power scheduling models.

GTES in terms of communication latency.

Power scheduling model. In this scenario, we calculated the median, standard deviation, and the confidence interval of SOC for three comparative power scheduling methods: BSoc, Equal Share, and FCFS. Fig. 4(a) shows the median, the 5th and the 95th percentiles of standard deviation of SOC when different number of EVs are considered in the power scheduling. We see that the median and the variance of the standard deviation of SOC follow BSoC<Equal Share<FCFS. The result means that our proposed power scheduling method in BSoC can balance EVs' SOC better than other two methods. The power scheduling model in BSoC considers balancing the SOC levels of EVs when they leave a charging lane and all EVs have approximately equal SOC. As a result, the deviation of SOC in BSoC is always small. The Equal Share power scheduling model only considers the equal distribution of energy and it does not pay attention to SOC. Thus, its deviation is moderate compared to other methods. The FCFS power scheduling model distributes power based on EV's arrival time and the deviation of FCFS power scheduling model from the median is large. Fig. 4(b) only shows the standard deviations of three methods. We can find that the standard deviation of our power scheduling method is lower than the standard deviations of other methods because of the reasoning mentioned above.

Vehicle-to-fog communication protocol. Fig. 5(a) and Fig. 5(b) show the experiment results from NS-3. Here, we calculated the average packet drop rate and the average packet delay with and without our channel allocation technique in current IEEE 802.11p protocol. We measured *the average packet drop rate* as the ratio of the number of packets dropped to the number of packets sent by all the EVs at each second. We find that the average packet drop rate in existing channel allocation technique is higher than our channel allocation technique when the number of EVs increases. Since EVs use their own channel for data transmission and the CSMA/CA approach is not used in our channel allocation technique, it causes less packet drop rate. Fig. 5(b) shows the results of average packet delay which also includes the delay of failed packets, which is basically the life span of failed packet. The average packet delay is affected by channel congestion. Basically, if the underlying communication channel is congested, it will increase the number of failed packets as well as average packet delay. In our efficient vehicle-to-fog communication protocol, the EVs use their own channels and the channel congestion is low. As a result, the average packet delay is low in our protocol.

IV. Related Work

Several works [7, 20–24] have discussed the design criterias for WPT systems. The studies in [20, 21] present different types of EVs with their different components and the research challenges based on existing technologies with their possible future impacts. Onar *et al.* [7] discussed several factors in the power transfer procedures with the consideration of highway surfacing materials and presented an overview of WPT magnetic field measurements. Li *et al.* [22] presented an analytic study of the technologies in the WPT area applicable to EV wireless charging. The work [24] presents the design of the electric components, an electromotive force shielding, and an optimized core structure with large air gaps for the WPT systems.

Another set of research work [23, 25–27] discuss the design and implementation issues of WPT systems. The study [25] presents the general design requirements and analysis of roadbed inductive power transfer systems. There are three different generic roadbed geometries based on: a long wire loop, a sectioned wire loops, and a spaced loops are used for the WPT systems. For a WPT system consists of novel core structure with narrow rail width, small pickup size and large air gap is presented in the study [23] with implementation of current source driven inductive power transfer system. Miller *et al.* [26] presented technical challenges posed by the dynamic charging of EVs – power pulsations. To mitigate the power pulsations inherent in coupling power from a series of embedded coils, the authors installed high-power capacitors at both the grid and in

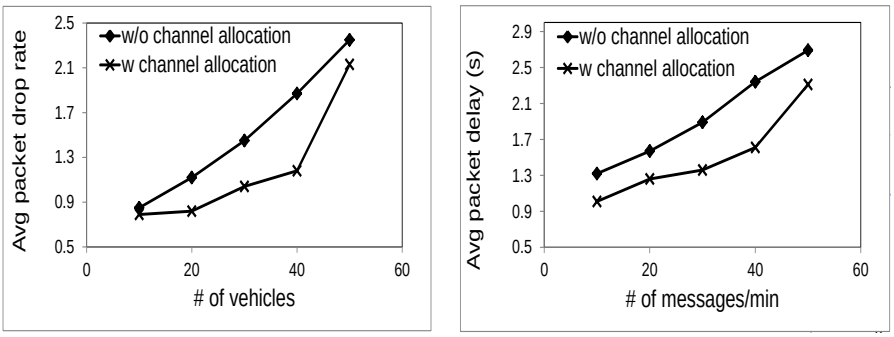

(a) Average packet drop rate

(b) Average packet delay

Figure 5: Comparison for channel allocation techniques.

vehicle to validate the benefit of power capacitors in energy storage systems. It creates ripple current to facilitate longer service life of the vehicle battery. Lee *et al.* [27] presented a dynamic model for the WPT system by applying the Laplace phasor transform to the first high-order IPTS. As a result, it creates a simple second-order equivalent circuit. With the help of this novel dynamic model, the maximum pickup current during the transient state is successfully identified where the current is relatively unchanged for various load resistances. The paper [28] presents the reduction of electromagnetic fields for the highly efficient wireless power transfer system. It also suggests a vertical magnetic flux type pickup coil with the optimized design parameters. Besides, passive metallic plate shield and active shield are proposed to minimize the leakage electromagnetic field from the wireless power transfer system in a (on-line) electric vehicle. However, none of these methods consider load balancing among different EVs which is a major challenge in WPT systems. The paper [29] presents an ongoing approach for transferring power from an antenna to another antenna in WPT system and it utilizes near-field antennas at resonance. The study by Ko and Jang [5] focuses two main factors for a WPT system: the battery size and the positions of power transmitters on the road. The authors presented the solution of an optimization model using particle swamp optimization technique to minimize the infrastructure cost with referenced to the battery size, the total number of power transmitters, and their allocation. Another study [6] presents a novel bidirectional WPT system for EV and V2G systems which includes loose magnetic coupling charging and discharging procedures. However, these methods do not consider the various number of EVs with their heterogeneous parameters while balancing the SOCs. In our method, we try to balance SOCs of EVs when the number EVs fluctuates and EVs share heterogeneous parameters. Our method also maintains high availability, high scalability, and low latency power distribution from grid to EVs.

V. Conclusion

This paper addresses the problem of how to let EVs have similar level of SOC to satisfy their energy requirements fairly in a WPT system for EVs in-motion. We proposed a WPT system namely *BSoC* for distributing power to in-motion EVs. There are three components in our proposed BSoC WPT system: i) fog-based power distribution architecture, ii) power scheduling model, and iii) efficient vehicle-to-fog communication protocol. First, to ensure the low latency, low computation overhead, and better localization, we used fog computing inside GSC. Second, to balance the SOCs of EVs, we presented and solved the power scheduling problem. Third, to reduce the network congestion load and to avoid hidden/exposed terminal problem, we devised an efficient vehicle-to-fog communication protocol where vehicles cooperate with GSC. We conducted extensive experimental study on three components of our proposed BSoC. Our experimental results confirmed that our proposed BSoC WPT system generates less communication latency, balanced SOC of EVs, and less packet drop rate. Currently, our proposed BSoC WPT system only considers balancing EVs' SOC. In the future, we will consider to satisfy the power needs for the entire routes from the sources to the destinations of EVs as an extension of our proposed power scheduling model.

Acknowledgements

This research was supported in part by U.S. NSF grants NSF-1404981, IIS-1354123, CNS-1254006, IBM Faculty Award 5501145 and Microsoft Research Faculty Fellowship 8300751.

References

[1] X. Cheng, X. Hu, L. Yang, I. Husain, K. Inoue, P. Krein, R. Lefevre, Y. Li, H. Nishi, J. G. Taiber, F.-Y. Wang, Y. Zha, W. Gao, and Z. Li, "Electrified vehicles and the smart grid: The ITS perspective," *IEEE Trans. on ITS*, vol. 4, no. 15, pp. 1388–1404, 2014.

[2] M. Buechel, J. Frtunikj, K. Becker, S. Sommer, C. Buckl, M. Armbruster, A. Marek, A. Zirkler, C. Klein, and A. Knoll, "An automated electric vehicle prototype showing new trends in automotive architectures," in *Proc. of ITSC*. IEEE, 2015, pp. 1274–1279.

[3] M. Honarmand, A. Zakariazadeh, and S. Jadid, "Optimal scheduling of electric vehicles in an intelligent parking lot considering vehicle-to-grid concept and battery condition," *Energy*, vol. 65, pp. 572–579, 2014.

[4] A. Diaz Alvarez, F. Serradilla Garcia, J. E. Naranjo, J. J. Anaya, and F. Jimenez, "Modeling the driving behavior of electric vehicles using smartphones and neural networks," *IEEE Intelligent Transportation Systems Magazine*, vol. 6, no. 3, pp. 44–53, 2014.

[5] Y. D. Ko and Y. J. Jang, "The optimal system design of the online electric vehicle utilizing wireless power transmission technology," *IEEE Trans. on ITS*, vol. 14, no. 3, pp. 1255–1265, 2013.

[6] U. K. Madawala and D. J. Thrimawithana, "A bidirectional inductive power interface for electric vehicles in V2G systems," *IEEE Trans. on IE*, vol. 58, no. 10, pp. 4789–4796, 2011.

[7] O. C. Onar, J. M. Miller, S. L. Campbell, C. Coomer, C. White, and L. E. Seiber, "A novel wireless power transfer for in-motion EV/PHEV charging," in *Proc. of APEC*. IEEE, 2013, pp. 3073–3080.

[8] J. Liu, L. Yu, H. Shen, Y. He, and J. Hallstrom, "Characterizing data deliverability of greedy routing in wireless sensor networks," in *Proc. of SECON*, 2015.

[9] Y. Lin and H. Shen, "Cloud fog: Towards high quality of experience in cloud gaming," in *Proc. of ICPP*, 2015, pp. 500–509.

[10] ——, "Autotune: game-based adaptive bitrate streaming in p2p-assisted cloud-based vod systems," in *Proc. of P2P*, 2015, pp. 1–10.

[11] L. Chen and H. Shen, "Consolidating complementary VMs with spatial/temporal-awareness in cloud datacenters." in *Proc. of INFOCOM*, 2014.

[12] C. Han, M. Dianati, R. Tafazolli, R. Kernchen, and X. Shen, "Analytical study of the IEEE 802.11p MAC sublayer in vehicular networks," *IEEE Trans. on ITS*, vol. 13, no. 2, pp. 873–886, 2012.

[13] J. Rios, P. Sauras-Perez, A. Gil, A. Lorico, J. Taiber, and P. Pisu, "Battery electric bus simulator-a tool for energy consumption analysis," in *Proc. of SAE*. IEEE, 2014.

[14] D. G. Luenberger and Y. Ye, *Linear and nonlinear programming*. Springer Science & Business Media, 2008, vol. 116.

[15] Z. M. Fadlullah, D. M. Quan, N. Kato, and I. Stojmenovic, "GTES: An optimized game-theoretic demand-side management scheme for smart grid," *IEEE Systems Journal*, vol. 8, no. 2, pp. 588–597, 2014.

[16] "Nissan-Leaf," http://www.nissanusa.com/electric-cars/leaf/versions-specs, [Accessed in March 2016].

[17] "Toyota-Prius," http://www.toyota.com/prius/features /exterior/1223/1224/1225/1226, [Accessed in March 2016].

[18] "Chevy-Volt," http://gm-volt.com/full-specifications, [Accessed in March 2016].

[19] Z. H. Mir and F. Filali, "LTE and IEEE 802.11p for vehicular networking: a performance evaluation," *EURASIP Journal on Wireless Communications and Networking*, vol. 2014, no. 1, pp. 1–15, 2014.

[20] Y. Hori, "Future vehicle society based on electric motor, capacitor and wireless power supply," in *Proc. of IPEC*. IEEE, 2010, pp. 2930–2934.

[21] S. Lukic and Z. Pantic, "Cutting the cord: Static and dynamic inductive wireless charging of electric vehicles," *IEEE Electrification Magazine*, vol. 1, no. 1, pp. 57–64, 2013.

[22] S. Li and C. C. Mi, "Wireless power transfer for electric vehicle applications," *IEEE Jorunal of Emerging and Selected Topics in Power Electronics*, vol. 3, no. 1, pp. 4–17, 2015.

[23] J. Huh, S. W. Lee, W. Y. Lee, G. H. Cho, and C. T. Rim, "Narrow-width inductive power transfer system for online electrical vehicles," *IEEE Trans. on PE*, vol. 26, no. 12, pp. 3666–3679, 2011.

[24] J. Shin, S. Shin, Y. Kim, S. Ahn, S. Lee, G. Jung, S.-J. Jeon, and D.-H. Cho, "Design and implementation of shaped magnetic-resonance-based wireless power transfer system for roadway-powered moving electric vehicles," *IEEE Trans. on IE*, vol. 61, no. 3, pp. 1179–1192, 2014.

[25] M. Yilmaz, V. T. Buyukdegirmenci, and P. T. Krein, "General design requirements and analysis of roadbed inductive power transfer system for dynamic electric vehicle charging," in *Proc. of ITEC*. IEEE, 2012, pp. 1–6.

[26] J. M. Miller, O. C. Onar, C. White, S. Campbell, C. Coomer, L. Seiber, R. Sepe, and A. Steyerl, "Demonstrating dynamic wireless charging of an electric vehicle: The benefit of electrochemical capacitor smoothing," *IEEE Power Electronics Magazine*, vol. 1, no. 1, pp. 12–24, 2014.

[27] S. Lee, B. Choi, and C. T. Rim, "Dynamics characterization of the inductive power transfer system for online electric vehicles by Laplace phasor transform," *IEEE Trans. on PE*, vol. 28, no. 12, pp. 5902–5909, 2013.

[28] S. Ahn and J. Kim, "Magnetic field design for high efficient and low EMF wireless power transfer in online electric vehicle," in *Proc. of EUCAP*. IEEE, 2011, pp. 3979–3982.

[29] T. Imura, H. Okabe, T. Uchida, and Y. Hori, "Wireless power transfer during displacement using electromagnetic coupling in resonance," *IEEJ Trans. on IA*, vol. 130, pp. 76–83, 2010.